TP13: The physics of crowding, packing and adsorbing

Supervisors: Dr Nick Jones, Dr Radek Erban, Dr Mason Porter
Candidate Number: 46755 **Word Count: 5185**

Abstract Polydisperse random sequential adsorption is one of few irreversible adsorption models for which exact results can be derived. The model was designed to describe the coating of viruses by polymers for use in gene therapy, but its applicability is more general. In many systems of interest, the arrangement of accessible adsorption sites is not known. An exact treatment of adsorption to a honeycomb lattice of sites is given and compared with the known square lattice results. The effects of lattice geometry are found to strongly depend on the polydispersity of the adsorbing particles. The existence of strong geometry dependencies suggests that disordered systems of adsorbing sites cannot be effectively modelled by regular lattices. A scheme is developed and tested in 1D, which improves the effectiveness of such modelling by transforming the polydispersity of the adsorbed particle mixture. Finally, simulation shows that existing analytical treatments cannot be applied to diffusion-driven polydisperse adsorption.

1 Introduction

Random sequential adsorption (RSA) is a process that involves the irreversible adsorption of particles onto a surface subject to the condition that no later particle overlaps a previously adsorbed one. RSA was first studied in the context of a 1D "car-parking problem" [1]. Since then a large variety of cases have been investigated. Examples include RSA in different numbers of dimensions; with continuous or discrete adsorption sites; with different sizes of adsorbing particles; and with interactions between adsorbed particles. [2][3]

RSA is a challenging problem in statistical mechanics because it is irreversible, has memory and involves spatial exclusion. The first of these ensures that the studied system is far from equilibrium; the second and third mean that the locations of the sites where the first particles are adsorbed affect the available end states. These complications mean that most studies are conducted by simulation, and exact results are known in only a minority of cases.

The most obvious use of RSA is in adsorption problems at liquid-solid interfaces, but the process has found applications in a diverse range of areas. RSA has been used to model crack formation [4], the deposition of energy in silicon detectors [5], and even the distribution of bird nesting sites [6]. Recently, a version of RSA called polydisperse-RSA (pRSA) has been motivated by a problem in gene therapy [7]. It is this version of RSA that will be the subject of this report.

Gene therapy involves the introduction of foreign genetic material into the cells of a patient. Viruses have evolved to do exactly this as efficiently as possible, so there is interest in using viruses as vectors. One particularly promising family of viruses are adenoviruses. Unfortunately, adenoviruses principally bind to the coxsackievirus adenovirus receptor (CAR) which is present on a great variety of cells that need not be targeted, and is not present on some cells that treatments hope to target. Additionally, the widespread nature of viruses of this type means that many patients will possess antibodies to it [8].

One category of proposed solutions to these problems involves coating the surface of the virus with polymers. The polymers serve to hide the virus from the body's immune system, and reduce the affinity for binding to the CAR receptor. In fact, by attaching appropriate ligands to the polymers, the virus may be

retargeted to specific cells with matching receptors [9].

pRSA describes the adsorption of variously sized semi-telechelic polymers (that is, polymers with only one binding group) to surfaces of discrete adsorbing sites. Each polymer adsorbs to one site (the occupied site), and the polymer tail sterically shields the sites it wriggles over (the covered sites) from further adsorption. At each time-step, a polymer size is selected according to a probability distribution, and an adsorbing site is selected at random. If the selected site is already occupied or covered, further adsorption does not take place; otherwise adsorption is successful. Two or more polymers may cover the same site, but only a single polymer can occupy a site.

It is worth noting that, despite the above description in terms of polymers, other adsorbing processes may be well-described by pRSA. In recognition of this possibility, subsequent discussion will be in terms of adsorbing 'particles'.

An advantage of pRSA is that it is analytically tractable. The average number of particles of each size adsorbed after a given number of time-steps is known in the case where the adsorption sites are arranged in a square lattice [7].

This report will attempt to answer three questions: 1) How does the distribution of adsorbed particles depend on the geometry of the lattice of adsorption sites? 2) Can anything be said about adsorption to lattices without a regular arrangement of sites? 3) In biological systems adsorption to a surface proceeds by diffusion. To what extent does diffusion of particles to the surface affect the foregoing analysis?

In Section 2, I adapt the existing square lattice methods to the new case of a honeycomb lattice. Comparison of the square and honeycomb results for a variety of adsorbing particle distributions allows the effects of lattice geometry on adsorption to be studied. Section 3.1 shows how a transformation of the adsorbing particle size distribution can reduce the problem of adsorption to a perturbed lattice to that of adsorption to an ordered one. For the sake of simplicity, a 1D lattice (i.e. a line of points) is considered. In Section 3.2 this technique is applied to look at the effect of thermally induced perturbations 'frozen into' a 1D lattice. In Section 4 the RSA model is coupled into a diffusion simulation.

2 Adsorption to a honeycomb lattice

An analytical solution for the adsorption, by pRSA, of particles onto the sites of a square lattice is given in [7]. This solution represents a modification of a method first described in [10] and [11]. In section 2.1 this method is adapted to the geometry of a honeycomb lattice. In section 2.2 the results from this analysis are compared with those for the square lattice case.

2.1 Formalism

Particles belong to one of three classes (Figure 1) – those large enough to cover only one site ('points'); those large enough to cover a site and its nearest neighbours ('Y particles'); and those large enough to additionally cover the next-nearest neighbour sites ('windmills'). Two particles in the same class may have different sizes, so a class is best understood to refer to the number of sites a particle covers, rather than to the particle size.

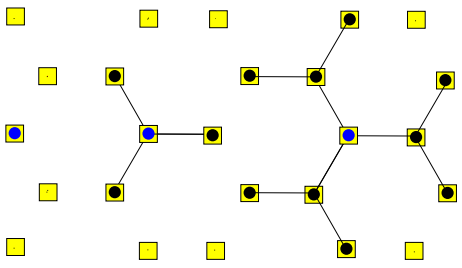

Figure 1: *From left to right: point, Y and windmill shapes formed by adsorption to the sites marked with blue circles ('occupied' sites). Yellow squares denote adsorption sites. The black circles are sites that will be 'covered' by each particle if they are not already occupied by another.*

In one RSA time-step a single attempt at adsorption is made. The probability that this will involve a Y particle is α, the probability that it will involve a windmill particle is β, and so the probability that it will involve a point particle is $\gamma = 1 - \alpha - \beta$.

Given a normalized distribution of adsorbing particle radii $Q(r)$, expressions for α and β can be found:

$$\alpha = \int_{r_a}^{r_b} Q(r)\ dr \quad , \quad \beta = \int_{r_b}^{\infty} Q(r)\ dr \quad (2.1)$$

where r_a is the distance between nearest neighbours, r_b is the distance between next-nearest neighbours, and $Q(r) = 0$ for $r \geq r_c$ where r_c is the distance to next-to-next-nearest neighbours.

Each site in the honeycomb lattice is identified by a pair of indices i, j. Inspection shows that not all lattice sites are equivalent: in fact there are two types related by a rotation of $\pi/3$. The windmill particle in Figure 1 is adsorbed to an *odd* site, and the central particle in Figure 2 is an *even* site. A careful choice of labelling system (Figure 2) allows each type of site to be immediately identified, and reduces the differences in their treatment. The set of nearest neighbour sites can be written as:

$$\chi_{i,j} = \{(i, j-1), (i, j+1), T_{i,j}\}$$

where:

$$T_{i,j} = \begin{cases} (i-1, j) & \text{if } i+j = \text{even} \\ (i+1, j) & \text{if } i+j = \text{odd} \end{cases}$$

Similarly, the set of next-nearest neighbour sites is:

$$\begin{aligned} S_{i,j} = &\{(i+1, j+1), (i+1, j-1), (i, j+2) \\ &(i, j-2), (i-1, j+1), (i-1, j-1)\} \end{aligned}$$

Each site can be in one of four states – occupied by a point, Y or windmill particle, or unoccupied. The configuration of an $M \times M$ lattice can be specified by a direct sum of these states at each site:

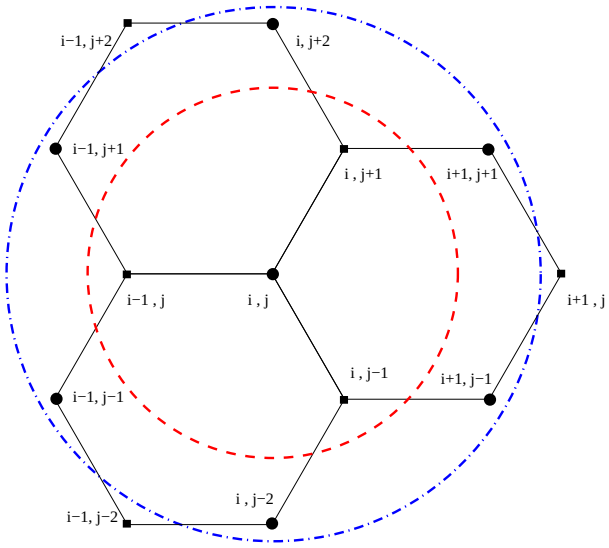

Figure 2: *A honeycomb lattice. In the notation of the text, the point i, j has $i + j =$ even. The inner circle encloses the nearest neighbour points. The outer circle encloses the next-nearest neighbour points.*

$$|\{v_{i,j}\}\rangle \in \bigoplus_{i,j=1}^{M} (\{|p\rangle, |Y\rangle, |w\rangle, |0\rangle\}) \quad (2.2)$$

The average state of the system, $|\psi(t)\rangle$, at any given time is a weighted sum of all possible configurations:

$$|\psi(t)\rangle = \sum_{\{v_{i,j}\}} P(\{v_{i,j}\}, t)|\{v_{i,j}\}\rangle \quad (2.3)$$

Note that, despite the suggestive notation, this is a classical process, and $P(\{v_{i,j}\}, t)$ is simply a probability.

Creation operators $\mathbf{A}^\dagger_{i,j}$, $\mathbf{B}^\dagger_{i,j}$ and $\mathbf{C}^\dagger_{i,j}$ are defined at each site for Y, windmill and point particles respectively. Their associated number operators are $\mathbf{N}^Y_{i,j}$, $\mathbf{N}^w_{i,j}$ and $\mathbf{N}^p_{i,j}$ respectively. These operators return 1 if the site is occupied by a particle of the given class, and return 0 otherwise. A fourth number operator $\mathbf{N}^v_{i,j}$ returns 1 if the site is unoccupied (this includes covered sites), and 0 otherwise.

Finally, an operator $\mathbf{R}_{i,j}$ is introduced such that $\mathbf{R}_{i,j}$ returns 0 when acting on a site that is

covered, and returns 1 otherwise. The equation describing pRSA can then be written as:

$$\frac{\partial}{\partial t}|\psi(t)\rangle = \frac{1}{M^2}\sum_{i,j=1}^{M}\mathbf{K}_{i,j}|\psi(t)\rangle \qquad (2.4)$$
$$\mathbf{K}_{i,j} = (\alpha\mathbf{A}_{i,j} + \beta\mathbf{B}_{i,j} + \gamma\mathbf{C}_{i,j} - \mathbf{N}^{v}_{i,j})\mathbf{R}_{i,j}$$

For the case of an initially empty lattice (i.e. at $t = 0$, $|\psi(t)\rangle = |\{0\}\rangle$) this has the solution:

$$|\psi(t)\rangle = \exp\left[\frac{t}{M^2}\sum_{i,j=1}^{M}\mathbf{K}_{i,j}\right]|\{0\}\rangle \qquad (2.5)$$

The average number of attached particles at time t is then:

$$N(t) = M^2\langle\{u\}|(\mathbf{N}^{p}_{1,1} + \mathbf{N}^{Y}_{1,1} + \mathbf{N}^{w}_{1,1})|\psi(t)\rangle$$

where $\{u\} = |u\rangle \oplus \cdots \oplus |u\rangle$ and $|u\rangle = |0\rangle + |Y\rangle + |w\rangle + |p\rangle$ is the 'universal state'. The choice of $i = 1, j = 1$ is arbitrary: all sites are assumed equivalent, so multiplying the result for one site by the number of points gives the full result.

By expanding the exponential in (2.5) into a power series and making use of relations between the operators (see [7] for details), this can be shown to be equivalent to:

$$N(t) = M^2\sum_{k=1}^{\infty}\frac{1}{k!}\left(\frac{t}{M^2}\right)^k(-1)^{k-1}A(k) \qquad (2.6)$$

$$A(k) = \sum_{s\in\mathcal{P}_k}[\alpha+\beta]^{\zeta(s)}\beta^{\omega(s)-\zeta(s)-1} \qquad (2.7)$$

where $\mathcal{P}_k$ is the set of sequences of k sites in which the first site is $i = 1, j = 1$ and each subsequent site is either already found earlier in the sequence, or is a neighbour or next-nearest neighbour of a site that is. The number of distinct sites in sequence s is $\omega(s)$. The number of distinct sites in sequence s that are nearest neighbours of sites that are found earlier in the sequence is given by $\zeta(s)$.

At this point it is useful to take the Laplace transform of (2.6) term by term.

$$\begin{aligned}\widehat{N}(u) &= \int_0^\infty N(t)e^{-ut}dt \\ &= \frac{-M^2}{u}\sum_{k=1}^{\infty}\left(-\frac{1}{uM^2}\right)^k A(k)\end{aligned} \qquad (2.8)$$

Equation (2.7) can now be rewritten as a sum over sequences with no repeated sites. The set of such sequences containing k sites is $\mathcal{G}_k$:

$$A(k) = F(k)\prod_{l=1}^{k}\left[1 + \left(-\frac{l}{uM^2}\right) + \ldots\right]$$

with

$$\begin{aligned}F(k) &= \sum_{s\in\mathcal{G}_k}[\alpha+\beta]^{\zeta(s)}\beta^{k-\zeta(s)-1} \\ &= \sum_{j=1}^{k}\phi^k_j[\alpha+\beta]^{k-j}\beta^{j-1}\end{aligned} \qquad (2.9)$$

where ϕ^k_j is the number of sequences in $\mathcal{G}_k$ satisfying the condition $j = k - \zeta(s)$.

Although the process leading to the values of ϕ^k_j is easy to understand, the values must be calculated numerically. The time that this takes grows rapidly with k. Table 1 contains these values for $k \leq 8$.

In [11] it is shown that (2.8) can be recast as:

$$\widehat{N} = \frac{M^2}{u}\int_0^1(1-x)^{uM^2}\sum_{k=1}^{\infty}\frac{(-x)^{k-1}}{(k-1)!}F(k) \qquad (2.10)$$

Finally, by taking the inverse Laplace transform (Bromwich integral) the result is $N(t) = \psi(x)$ where:

$$x(t) = 1 - \exp\left[-\frac{t}{M^2}\right] \qquad (2.11)$$

$$\psi(x) = M^2\sum_{k=1}^{\infty}\frac{(-1)^{k-1}x^k}{k!}F(k) \qquad (2.12)$$

Table 1: *Table of values of* ϕ_j^k *for* $k = 1, 2, \ldots, 8, \quad j = 1, \ldots, k$

ϕ_j^k	$j=1$	$j=2$	$j=3$	$j=4$	$j=5$	$j=6$	$j=7$	$j=8$
$k=1$	1	–	–	–	–	–	–	–
$k=2$	3	6	–	–	–	–	–	–
$k=3$	12	54	48	–	–	–	–	–
$k=4$	60	426	840	468	–	–	–	–
$k=5$	360	3432	10944	13272	5328	–	–	–
$k=6$	2472	29520	131172	256488	221016	68928	–	–
$k=7$	18912	272568	1557012	4284816	5908620	3914916	994464	–
$k=8$	158544	2691912	18846324	67503996	131005572	137901120	73838136	15781920

As each class of particle can adsorb to every site of the lattice with equal chance of success, the number of attached particles of different classes can easily be calculated from $N(t)$:

$$N^Y(t) = \alpha N(t) \qquad N^w(t) = \beta N(t)$$
$$N^p(t) = \gamma N(t) \tag{2.13}$$

The expression given for $\psi(x)$ converges slowly. Wynn's epsilon method [12] is used to accelerate convergence. In practice the series converges well with the input of the first eight terms, but convergence is not guaranteed.

2.2 Application to the honeycomb lattice

The general features of the resulting adsorption process are easy to predict. At first, the adsorbing surface is empty, so almost every adsorption attempt is successful. As time progresses, the surface becomes saturated and the rate of adsorption of additional particles decreases.

The method used gives the mean value of $N(t)$ at all t. There is no reason to suppose that this is the modal value, so it is worth investigating the spread of values of $N(t)$ from many simulations. Figure 3 shows smoothed histograms (each bin is replaced with the average of itself and the bins on either side) from 5000 runs to saturation on a 200×200 site lattice in both the square and honeycomb cases. Reassuringly, the derived values sit within broad peaks. The widths of the peaks are dependent on α, β and γ (this can be seen from the $\gamma = 1$ case), but unfortunately no relation for them is known.

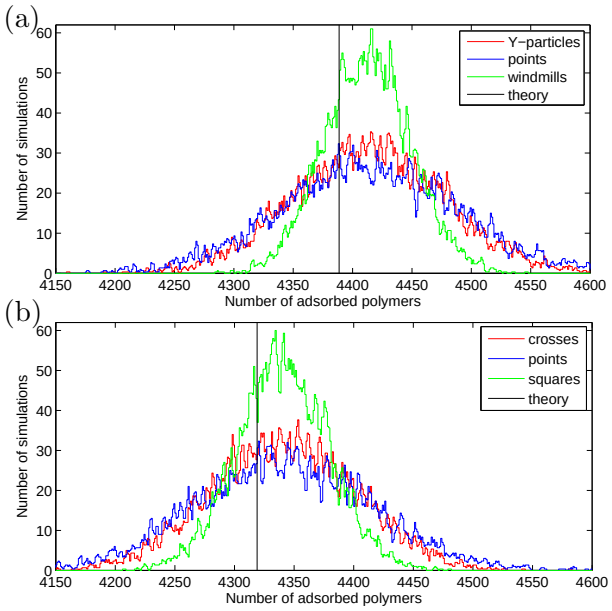

Figure 3: *Smoothed curves of the number of particles of different classes adsorbed at saturation for a) honeycomb lattice and b) square lattice ('crosses' and 'squares' are the square lattice equivalents of Y-particles and windmills respectively). To aid comparison* $\alpha = \beta = \gamma = 1/3$.

Plots of this sort caution against overzeal-

ous use of (2.11) and (2.12). The derivation of these expressions means that they are accurate only for large M^2, and are limited by the power of the algorithm used to accelerate convergence. The calculated values of $N(t)$ at saturation on a 200×200 site honeycomb (square) lattice are 0.55% (0.50%) below the experimental mean for all classes of particle; for a 100×100 site lattice, the calculated values are $\sim 1.0\%$ too low in all cases.

It is instructive to compare the results of adsorption to the honeycomb lattice with their square lattice equivalents. Figure 4 shows the difference at saturation in the mean number of particles adsorbed on a 100×100 site lattice of each type for all values of α and β.

The figure has several intriguing features. Firstly, one can see that some values of α and β have almost the same number of adsorbed particles of each class. This is trivially true for $\alpha = \beta = 0$, but also appears to hold along the contour best described by the yellow band in the bottom half of Figure 4(d).

A second point of note is the extreme values of the plots. Varying α, β and γ corresponds to varying the concentrations of different classes of adsorbing particle. Certain concentrations have a large sensitivity to the geometry of the lattice e.g. at $\alpha = 0.5$, $\beta = 0$, whereas others do not. In terms of the virus coating problem, this suggests that the distribution of the virus binding sites may greatly affect the composition of the resulting coat.

Figure 4(c) shows another interesting result – a honeycomb lattice adsorbs either approximately the same or more nearest-neighbour particles than a square lattice for all values of α, β and γ. This result may not at first seem surprising: a honeycomb lattice site has three nearest neighbours, whereas a square lattice site has four, so on equally-sized lattices one would naively expect more honeycomb Y-particles. However, this cannot be the whole explanation – the same argument applied to Figure 4(d) fails to account for the higher number of windmill particles. The result is instead related to the way that cross, square and point particles may be tessellated in the two cases.

3 Perturbed Lattices

The strong effects of lattice geometry on the numbers of each class of particle that are adsorbed suggests the need for a scheme to treat disordered lattices. It seems likely, for example, that adsorption to sites arranged in an approximately square lattice cannot be modelled by adsorption to sites in a regular square lattice. Here I consider the case of a perturbed lattice – that is, a lattice whose sites have been displaced from a regular arrangement by a small amount, the magnitude of which follows a well-defined probability distribution. A one dimensional lattice (a line of points) is considered for simplicity.

The aim of this section is to illustrate a scheme by which approximate expressions for α and β analogous to those in (2.1) can be found for a perturbed lattice. It was stressed in Section 2 that these probabilities should be interpreted in terms of the number of sites that each particle covers, rather than each particle's size. This interpretation is necessary in the perturbed case, where a small particle may adsorb to cover many closely-spaced sites.

3.1 One Dimension

Each lattice site falls on a line, and is spaced a distance a from its neighbours. Each site is then displaced along the line by an amount ξ (which varies from point to point and may be negative) from this equilibrium position. The displacements are described by a probability distribution $\mathrm{P}(\xi)$.

In pRSA we randomly select a site to be adsorbed to and then look at the positions of the n^{th} nearest sites to the left and right ($n = 1$ corresponds to the nearest neighbours, $n = 2$ the next-nearest neighbours and so on). If the adsorbing particle has 'radius' z, then any sites closer than z are considered covered. Unfortunately, as the site that will be adsorbed to has also been perturbed, if the nearest neighbour to the left is found to be very close, then the probability of the one to the right being far away increases – the probability of cover-

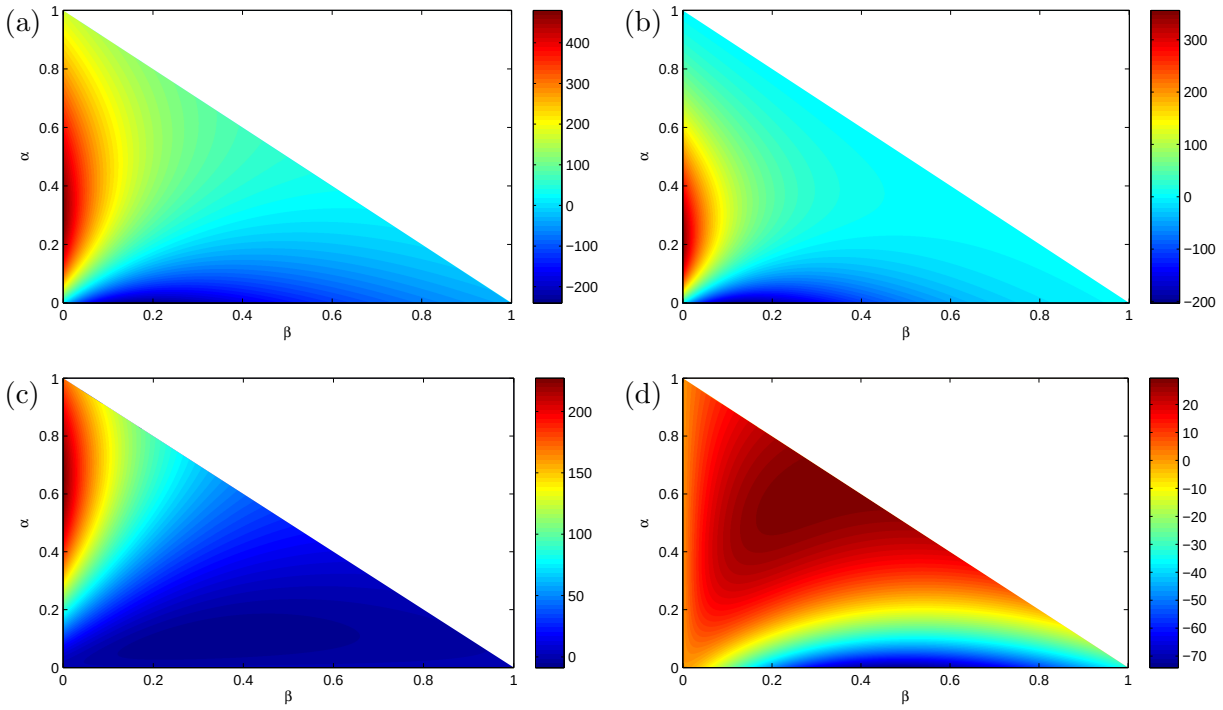

Figure 4: *Colour plots of the calculated average additional number of particles adsorbed onto a honeycomb lattice with respect to a square lattice for all α, β and γ. Note that the scaling for each plot is different. a) Total number of adsorbed particles b) Number of particles that cover one point only c) Number of particles that cover nearest neighbours d) Number of particles that cover both nearest and next-nearest neighbours.*

ing two initially equidistant sites on the line is not the square of the probability of covering one.

Exact results are obtained by taking a convolution of the probability distribution for each site on the line. I will restrict the discussion here to three convolutions. The probability of two sites, initially equidistant from the adsorbing site, being perturbed such that the first ends up a distance v_1, and the second a distance v_2 further away from the perturbed adsorbing site is:

$$H(v_1, v_2) = \int_{-\infty}^{\infty} P(\xi)\ P(v_1 + \xi) \times P(v_2 + v_1 + \xi)\ d\xi \quad (3.1)$$

Let the distribution of adsorbing particles with radius z be $Q(z)$. The probability, R_n^m, that m n^{th} nearest neighbours are occupied can now be directly calculated.

$$R_n^2 = \int_0^{\infty} Q(z) \int_{-z-na}^{z-na} \int_{-z-na}^{z-na} H(v_1, v_2)\ dv_1 dv_2 dz$$

$$R_n^1 = 2 \int_0^{\infty} Q(z) \int_{-z-na}^{z-na} \left(\int_{z-na}^{\infty} + \int_{-\infty}^{-z-na} \right) \times H(v_1, v_2)\ dv_1 dv_2 dz$$

$$R_n^0 = 1 - R_n^2 - R_n^1 \quad (3.2)$$

The factor of 2 arises in R_n^1 because there are 2 ways of occupying one site of a pair.

For most $Q(z)$, equivalent expressions to the above with more than 3 convolutions become extremely time-consuming to calculate. This is the reason that the 3 convolution case has been focussed on. Nevertheless, taken together with the approximation that pairs of sites behave independently of each other, this is found to

describe physical systems under sizeable perturbations.

3.2 Example

As a physical, albeit unrealistic, example, imagine there to be some restoring force holding each site in position. Then for small displacements the potential is parabolic, and so the probability distribution for displacements due to thermal agitation is, via a partition function:

$$P(\xi) \approx \sqrt{\frac{b}{\pi}} e^{-b\ \xi^2} \tag{3.3}$$

Here, b is a constant that depends on the temperature of the system and the strength of the restoring force. In what follows this 'heat motion' is assumed to be frozen into the lattice. The approximation is due to the parabolic potential being assumed to hold for all ξ. For sufficiently large values of b, this is a good description. Calculating (3.1) for this case gives:

$$H(v_1, v_2) \approx \sqrt{\frac{1}{3}} \frac{b}{\pi} e^{\frac{-2b}{3}(v_1^2 + v_2^2 - v_1 v_2)}$$

Once a choice of particle size distribution, $Q(z)$, has been made, the values of R_n^m can be calculated using (3.2). For simplicity, I will take the unperturbed lattice spacing to be $a = 1$, and $Q(z)$ to be a uniform distribution for $z = [0, 1]$. Recall that z is the analogue of a 'radius', so the largest particles are 2 units long.

The first few values of R_n^m for $b = 2$ are given in Table 2. The $n = 0$ case allows for the fact that every adsorbed particle covers at least one site. As a first approximation, probabilities for different n are assumed to be independent. Hence, the probability that any given number of sites are covered or occupied can be determined from the table. For example, the probability, $\Lambda(3)$ that 3 sites are covered or occupied is equal to the sum of the probabilities that both particles of one pair are covered and neither particle from any other pair, and the probabilities that one particle from each of two pairs is covered and no particle from the third pair.

An unperturbed lattice with probability $\Lambda(d)$ of adsorbing a particle that covers d sites should then adsorb in the same way as the perturbed lattice.

	Number of occupied sites, m		
n	0	1	2
0	0	1	0
1	0.65100	0.23334	0.11566
2	0.95699	0.03772	0.00529
3	0.99906	0.00092	0.00003

Table 2: *Probabilities R_n^m, that none, one or both of a pair of sites are covered for $b = 2$, and for up to next-to-next-nearest neighbours.*

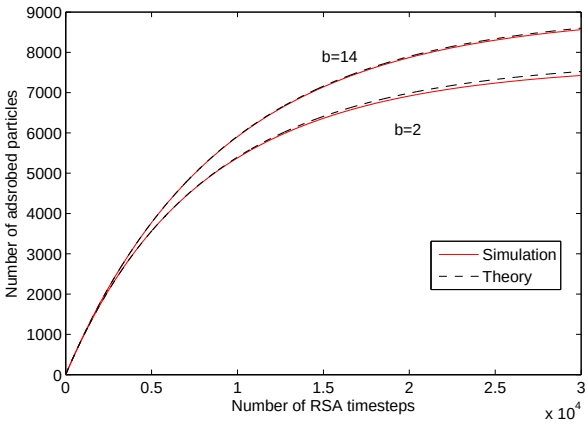

Figure 5: *Comparison of theory with simulation for two different magnitudes of perturbation. The simulation values are the averages of 250 runs of pRSA on 10,000 sites perturbed according to (3.3). The theoretical values are the averages of 250 runs on an unperturbed lattice with the probabilities of a particle covering a given number of sites calculated as described in the text. An unperturbed lattice would saturate after 10,000 adsorptions.*

In Figure 5, the number of adsorbed particles is shown for the perturbed lattice and its 3-convolution equivalent for $b = 2$ and $b = 14$. Unsurprisingly, the approximation worsens as b decreases: for large perturbations more convolutions are required. For $b = 2$ the theory

result at saturation is 1.3% higher than the simulation one. For $b = 14$ the theory result is 0.45% too high at saturation. In constructing the theoretical results, values of $\Lambda(d)$ were computed for $d \leq 7$ using the values of R_m^n for $n \leq 3$.

4 Diffusion

Many biological processes proceed by diffusion onto an adsorbent surface. Consider a solution of adsorbing particles of a single type. As particles are adsorbed to the surface, the concentration next to the surface drops – further adsorption is unlikely until more adsorbing particles diffuse in. This means that each RSA time step corresponds to a different amount of real time.

A method is described in [13] for coupling the time-step used in RSA to a real-time diffusion problem. In this section I will apply this method to the case of several sizes of particles. In this case, adsorption of a particle of one type leads to a decrease in the concentration of that type of particle, but the concentration of other types of particles is unaffected. In the language of Section 2, α, β and γ become time dependent.

I study adsorption, by pRSA, from an initially well-mixed polydisperse solution to an infinite plane at $y = 0$ (in Cartesian coordinates). The symmetry of this problem ensures that the concentration is uniform in the x-z plane. Consequently, the diffusion equation for this system is:

$$\frac{\partial c_i(y,t)}{\partial t} = D_i \frac{\partial^2 c_i(y,t)}{\partial y^2} \qquad (4.1)$$

where for particle species i, D_i is the diffusivity, and $c_i(y,t)$ is the concentration at time t a distance y from the adsorbing surface.

Ref. [13] shows that RSA can be coupled into this system via the following Robin boundary condition:

$$\frac{\partial c_i(0,t)}{\partial y} = \theta_i(t) \frac{2P}{\sqrt{D_i \pi}} c_i(0,t) \qquad (4.2)$$

In this condition P is related to the timescale over which a single particle is adsorbed and $\theta_i(t)$ is a function that takes the values 0 or 1 at all times. When an adsorption attempt by a particle of species i is successful $\theta_i(t) = 1$ until an unsuccessful attempt is made. Conversely, when an attempt is unsuccessful $\theta_i(t) = 0$ until a successful attempt is made. Attempts are made whenever $\kappa(t)$ increases by one unit, where $\kappa(t)$ is given by:

$$\kappa(t) = \left\lfloor \int_0^t \frac{2P\sqrt{D_i}}{\sqrt{\pi}} c_i(0,t) dt \right\rfloor \qquad (4.3)$$

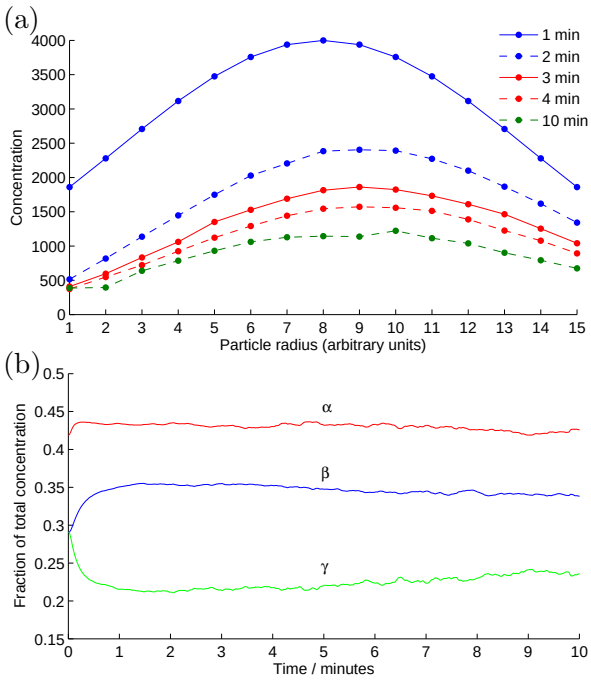

Figure 6: *Concentration and adsorption probability curves for diffusion onto a* 100×100 *site square lattice. The curves are from 0.02 mm above the adsorbing boundary. At the end of the simulation the lattice is 91% occupied. a) The peak of the concentration curve initially shifts towards slower diffusing particles, and then begins to flatten out. b) The parameters* α, β *and* γ *show time dependence.*

Figure 6 shows the results of a simulation of diffusion driven adsorption onto a 100×100 site square lattice with the above boundary condition and the additional conditions:

$$c_i(y,0) = c_i(\infty,t) = 4000\ e^{(-(8-i)/8)^2)} \quad (4.4)$$

A total of 15 particle sizes are simulated ($i = 1 \ldots 15$). The condition (4.4) thus describes a normal distribution peaking at $i = 8$. Particle species $i = 1 \ldots 5$ adsorb to a single point, species $i = 6 \ldots 10$ adsorb to cover nearest neighbours, and species $i = 11 \ldots 15$ also cover next-nearest neighbours. All particles are non-interacting.

For simplicity, $P = 1s^{-1/2}$, and the boundary condition at infinity is moved to 1 mm above the adsorbing surface. The concentrations have dimensions of mm^{-1} above the adsorbing area, and a simple scaling relation is used for the diffusivity:

$$D_i = \frac{5 \times 10^{-5}}{i} \quad mm^2\ s^{-1} \qquad (4.5)$$

All of the above values have approximately the correct order of magnitude to describe long molecules adsorbing onto sites spaced $\sim nm$ at a concentration of $\sim g/l$.

Figure 6b) shows that α, β and γ change rapidly at early times. This behaviour means that in this case (2.5) cannot be used to describe the time-evolution of the system. Great care should be taken in applying the results of Section 2 to diffusion-driven adsorption processes.

Despite this caveat, Section 2 is still applicable to many laboratory situations, where the solution can be shaken to ensure that it is always well-mixed.

5 Conclusions

pRSA is one of very few RSA models for which analytical results can be derived. In this report, several features of pRSA have been investigated – in particular the model's dependency on lattice type and particle distribution.

The relation of pRSA to other RSA algorithms e.g. hard sphere adsorption, is not a simple one, and it is unlikely that the results found here can be generalised. Fortunately, however, pRSA has applicability to real-life systems, as its original motivation of virus-coating suggests. The utility of the present analytical treatment would be greatly increased if the variance of the number of adsorbed particles was known, rather than just the mean.

One surprising result from this work is that there is a group of polydisperse distributions under which the adsorption properties of a lattice are geometry independent. It would be interesting to see whether such groups generally occur, or are limited to the square and honeycomb case.

It is also apparent that a small change in a polydisperse distribution can lead to a substantially different coating if the geometry of the adsorbing surface is not known. This variation in particle adsorption between different lattices at different concentrations raises the intriguing possibility that nature may have got there first. For example: do structures exist that are optimised to pick out a certain sized reactant by statistical, rather than specialised chemical processes?

The effects of varying lattice geometry suggested the need for an analytical scheme to treat disordered lattices – which are much more likely to occur in biological systems. The applicability of the approach presented here may be wide – there is no need to physically motivate the probability distribution leading to disordering, so it may be possible to characterise a distribution by direct measurement of adsorption site displacement.

Whilst results were presented for a simple 1D case, it should be possible to generalize the results to two dimensions. It is, however, likely that the resulting integrals will be extremely time-consuming to solve except for the simplest particle size distributions.

It is an unsurprising, but previously unreported result that polydisperse diffusion-driven adsorption cannot be modelled by present analytical treatments. It is hoped that investigation of the time dependence of particle concentration in a wider range of simulations will allow an effective modification of the existing treatment to be derived.

References

[1] Rényi, A. *Publ. Math. Inst. Hung. Acad. Sci.* **3**, 109 (1958).

[2] Evans, J. W. Random and cooperative sequential adsorption. *Reviews of Modern Physics* **65**, 1281–1329 (1993).

[3] Talbot, J., Tarjus, G., Tassel, P. R. V. & Viot, P. From car parking to protein adsorption: an overview of sequential adsorption processes. *Colloids and Surfaces A: Physicochemical and Engineering Aspects* **165**, 287 – 324 (2000).

[4] Gromenko, O., Privman, V. & Glasser, M. Random sequential adsorption model of damage and crack accumulation: Exact one-dimensional results. *Journal of Computational and Theoretical Nanoscience* **5**, 2119–2123 (2008).

[5] Subashiev, A. & Luryi, S. Random sequential adsorption of shrinking or expanding particles. *Phys. Rev. E* **75**, 011123 (2007).

[6] Tanemura, M. & Hasegawa, M. Geometrical models of territory. *Journal of Theoretical Biology* **82**, 477–496 (1980).

[7] Erban, R. & Chapman, S. On chemisorption of polymers to solid surfaces. *J. Stat. Phys.* **127**, 1255–1277 (2007).

[8] Mizuguchi, H. & Hayakawa, T. Targeted adenovirus vectors. *Human Gene Therapy* **15**, 1034–1044 (2004).

[9] Fisher, K. *et al.* Polymer-coated adenovirus permits efficient retargeting and evades neutralising antibodies. *Gene Therapy* **8**, 341–348 (2001).

[10] Dickman, R., Wang, J. & Jensen, I. Random sequential adsorption: series and virial expansions. *J. Chem. Phys.* **94**, 8252–8257 (1991).

[11] Fan, Y. & Percus, J. Asymptotic coverage in random sequential adsorption on a lattice. *Phys. Rev. A* **44**, 5099–5103 (1991).

[12] Wynn, P. On a device for computing the $e_m(s_n)$ transformation. *Mathematical Tables and Other Aids to Computation* **10**, 91–96 (1956).

[13] Erban, R. & Chapman, S. Time scale of random sequential adsorption. *Phys. Rev. E* **75**, 041116 (2007).